JOURNAL OF MATERIALS SCIENCE 24 (1989) 2285–2294

Precipitate formation in Nimoncic PE16

R. M. BOOTHBY, G. C. CATTLE, T. L. BRYDON*
Materials Development Division, Harwell Laboratory, UKAEA, Harwell, Didcot, Oxfordshire, UK

Besides γ' and the matrix, seven other phases have been identified in Nimonic PE16. Four of these, MC, TiN, $M_4C_2S_2$ and M_3B_2 are primary phases. The carbide $M_{23}C_6$ precipitates intergranularly on ageing and is unstable above 950° C. Laves phase is formed on long-term ageing at 600 to 750° C and M_6C at 600 to 700° C. The formation of Laves and M_6C is accelerated by cold working and by pre-ageing at 700° C prior to lower temperature exposure. A detailed assessment of γ' precipitation at 750° C has shown that, for both intragranular and grain-boundary γ', the precipitate diameters increase with ageing time, t, according to an approximate $t^{1/3}$ relationship. The γ' volume fraction increases continually during ageing for times up to 6000 h at 750° C. The composition of γ' is dependent on ageing temperature, the ratio of aluminium to titanium increasing as the temperature is reduced.

1. Introduction

The structure and properties of Nimonic PE16 have been widely investigated, both from the fundamental viewpoint of γ' strengthening [1] and in studies relating to reactor core component applications, e.g. [2–4]. However, several aspects of the precipitation behaviour of PE16 have not been fully examined and a number of uncertainties have arisen in the literature. For example, the nature of the phases responsible for boundary pinning during abnormal grain growth has been disputed [5, 6], and the time and temperature dependence of the γ' volume fraction formed on ageing is unclear [2, 7–9]. Moreover, the presence of some primary phases and the formation of some carbide and intermetallic phases on ageing has not been well documented. In order to clarify this situation a detailed study of precipitate formation and stability in PE16 at temperatures ranging from 1050 to 600° C has been carried out. This study encompasses work on the identification of the primary phases MC, MN, $M_4C_2S_2$ and M_3B_2 (where M signifies metallic elements), and on the formation of $M_{23}C_6$, MC, M_6C, Laves phase and γ' on ageing.

2. Experimental details

2.1. Materials and heat treatments

The analysis of the Nimonic PE16 alloy (cast DAA 766) used throughout this study is given in Table I. The alloy was hot rolled at 1050° C from 13 mm diameter rod to 0.762 mm strip, and subsequently cold rolled to 0.635 mm. The material was then divided into three batches as follows:

(a) solution treated (ST) at 1050° C for 0.25 h in flowing argon and water quenched; then used for ageing experiments at 600 to 950° C.

(b) ST as (a) and pre-aged 16 h at 700° C; then used to examine the high-temperature stability of $M_{23}C_6$ and in ageing experiments at 600 and 650° C.

(c) retained in the cold worked (CW) condition for ageing experiments at 600 to 750° C.

All ageing treatments were carried out with the specimens sealed in argon-filled silica capsules and were terminated by water quenching of the capsules. Ageing times of 4000 h or more were achieved at 750° C and below, but shorter periods were deemed sufficient at higher temperatures.

2.2. Electron microscopy

Characterization of the precipitates was mainly carried out using carbon extraction replicas, although thin foils of selected specimens were also prepared. Carbides and all other precipitated phases except γ' were extracted by electrolytic etching in 10% HCl/methanol followed by carbon deposition and stripping of the replicas in the same solution. The γ' phase was extracted by electrolytic etching and stripping of the replicas in 10% oxalic acid. In addition, surface replicas, showing the location of γ' precipitates intersecting the specimen surface but not extracting them, were prepared by etching in oxalic acid but stripping in HCl/methanol. Thin foils were prepared from 3 mm diameter spark-machined discs by electropolishing in a static bath of 10% perchloric acid/20% glycerol/70% ethanol at room temperature, or alternatively by jet electropolishing in 5% perchloric/methanol cooled to below −50° C.

Replicas and foils were examined in a Philips EM400T transmission electron microscope (TEM) operating at 100 keV, and the phases were identified by electron diffraction and using an Edax SW9100/60 energy dispersive X-ray (EDX) analysis system. In addition, electron energy loss spectroscopy (EELS) of some phases was carried out using foil specimens (to avoid the inevitable carbon signal from replicas) in a 300 keV Philips EM430T microscope interfaced to a Gatan spectrometer and Link Systems software.

* *Permanent address*: CEGB, Berkley Nuclear Laboratories, Berkley, Gloucestershire, UK.

TABLE I Analysis (wt %) of Nimonic PE16 Cast DAA 766

Ni	Fe	Cr	Ti	Al	Mo	Zr	Mn	Si	C	N	B	S	P
43.5	34.3	16.5	1.18	1.15	3.17	0.02	0.05	0.15	0.051	0.020	0.0018	0.005	0.007

Quantitative assessments of γ' particle size were made from extraction replicas, and of the number of precipitates per unit area, N_A, from surface replicas. Precipitate diameters were measured using a digitizing tablet linked to a microcomputer. The mean precipitate diameter, $\bar{d}$, the diameter of a precipitate of average volume, d_v, given by

$$d_v = \left(\sum_{i=1}^{n} d_i^3 / n \right)^{1/3} \quad (1)$$

where d_i are the individual precipitate diameters and n is the number of precipitates measured, and the size distribution in terms of $(d_i/\bar{d})$ were determined from measurements of 500 precipitates. Assuming the extracted precipitates to constitute a true volume distribution (see Section 3.3 for discussion of this point), the number of precipitates per unit volume, N_V, is given exactly by [10, 11]

$$N_V = N_A/\bar{d} \quad (2)$$

and the volume fraction, f, by

$$f = (\pi/6) d_v^3 N_V \quad (3)$$

The size of grain boundary γ' particles was assessed separately from intragranular ones. Because the grain-boundary precipitates were not generally spherical, the parameter chosen for measurement was the maximum particle width parallel to the boundary direction. The average size of the grain boundary γ', d_b, was determined from measurements of 100 particles. The composition of the γ' phase was examined by EDX analyses, with ten determinations per specimen for each of intra- and inter-granular precipitates.

3. Results and discussion

Besides γ' and the matrix, seven other phases (some with compositional variants) were encountered in Nimonic PE16. The structures and lattice parameters of these phases are listed in Table II.

3.1. Primary phases

The most abundant primary phases in PE16 were found to be the Ti–Mo carbide MC and the nitride TiN. EDX and EEL spectra of these phases are shown in Fig. 1. Although the carbide and nitride are mutually soluble [12], the EEL data indicate that the thermal origins of the two phases are sufficiently distinct for inter-diffusion not to occur.

TABLE II Structures and lattice parameters of phases in PE16

Phase	Structure	Lattice parameters (nm)
MC	fcc	0.43
TiN	fcc	0.42
$M_4C_2S_2$	hexagonal	$a = 0.34$, $c = 1.21$
M_3B_2	tetragonal	$a = 0.585$, $c = 0.315$
$M_{23}C_6$	fcc	1.06
M_6C	diamond cubic	1.09
Laves	hexagonal	$a = 0.48$, $c = 0.78$

Less abundant primary phases were the carbo-sulphide $M_4C_2S_2$ and the boride M_3B_2. Although neither phase has been reported previously in PE16, both are known to occur in nickel-based superalloys [13, 14]. EDX examination of the carbo-sulphide, Fig. 2, revealed a range of compositions with both zirconium-rich and titanium-rich versions present. (Note that the copper signals in these EDX spectra and in others taken from extraction replicas arise from the specimen support grids rather than the particles.) EDX analysis showed the boride to be a Mo–Cr-rich phase, and EELS confirmed the presence of boron, Fig. 3.

The beneficial influence of boron and zirconium additions on the creep properties of nickel-based alloys, including PE16 [15], is well known although not completely understood [16–18]. However, it is generally recognized that boron and zirconium counteract the effects of deleterious grain-boundary segregants including sulphur. Thus, the incorporation of sulphur into zirconium-rich primary inclusions is likely to be of benefit, but the formation of borides – preventing boron segregation to grain boundaries – is not.

3.2. Precipitation during ageing

The kinetics of grain-boundary carbide formation during short-term (up to 1 h) ageing of PE16 have been investigated in detail by Faulkner and Caisley [19], and consequently the present study was directed towards establishing the nature of precipitation at longer times. Isothermal ageing for periods of 4 h or more resulted in grain-boundary precipitation of the chromium-rich carbide $M_{23}C_6$ at 600 to 850° C and of MC at 850 to 950° C. The upper limit for $M_{23}C_6$ formation of 850° C is about 50° higher than indicated by Faulkner and Caisley's work. Two compositional variants of $M_{23}C_6$ were detected by EDX analyses. In addition to chromium, the more usual form of $M_{23}C_6$ contained some molybdenum and small amounts of iron and nickel (Fig. 4a). The second, much rarer, type was richer in iron and free from molybdenum and nickel (Fig. 4b).

In order to examine Randle and Ralph's assertion that the solvus temperature for $M_{23}C_6$ in PE16 is as high as 1120° C [6], specimens pre-aged for 16 h at 700° C were subjected to higher temperature annealing. $M_{23}C_6$ formed at 700° C was partially retained during a subsequent 16 h exposure at 900° C but completely replaced by MC in 4 h at 950° C. The $M_{23}C_6$ precipitates in 16 h/700° C aged PE16 were also fully dissolved during re-solution treatments of 1 h at 1000° C and 0.25 h at 1050° C. The fact that $M_{23}C_6$ is unstable in PE16 at 950° C and above is contrary to the view that this phase can influence grain-growth behaviour during solution treatment [6]. As concluded previously [5], only primary phase particles can resist dissolution and pin the grain boundaries during high-temperature annealing.

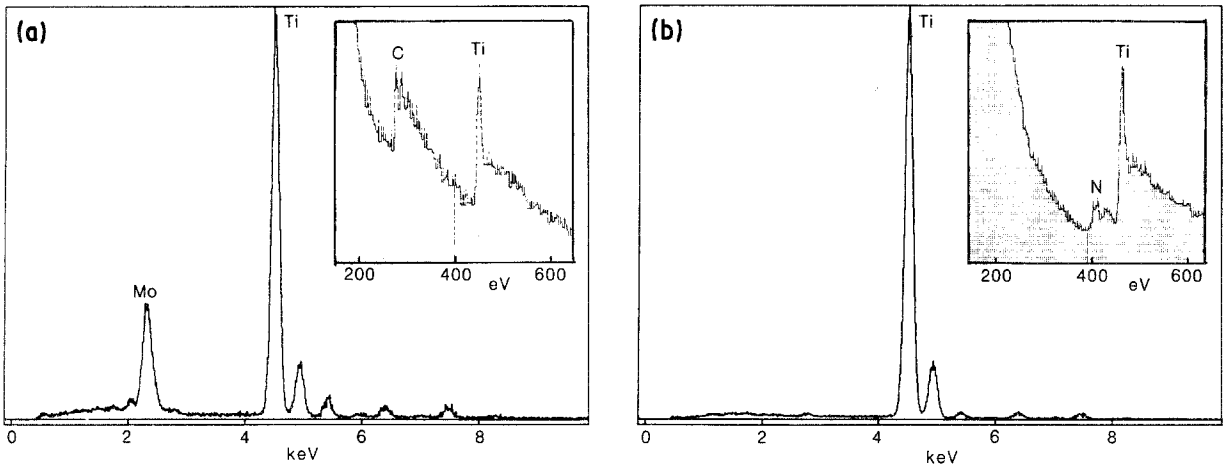

Figure 1 EDX and EEL spectra from (a) MC and (b) TiN.

In addition to $M_{23}C_6$, Laves phase and M_6C were also formed at grain boundaries on longer term ageing at the lower temperatures. Both phases were enriched in molybdenum and silicon, the Laves phase being characterized by a heavily faulted structure (Fig. 5) and appreciable levels of iron, chromium and nickel (Fig. 6), and M_6C by a high nickel content (Fig. 7). Time-temperature–precipitation curves for Laves phase and M_6C are shown in Figs 8 and 9, respectively. Laves phase formation was not observed above 750° C nor M_6C above 700° C. The formation of both phases was accelerated by pre-ageing for 16 h at 700° C (STA condition) prior to lower temperature exposure and by cold working. Intragranular precipitation of Laves phase, in an acicular form generally nucleated on MC particles, was observed after 4000 h at 650 and 700° C (Fig. 10).

Laves phase formation has been noted previously in PE16 aged for 20 000 h at 600 and 700° C [20] and in cold-worked PE16 which underwent partial recrystallization in 3000 h at 750° C [21]. Being a brittle intermetallic phase, Laves precipitation can be expected to result in degradation of mechanical properties [22]. The loss of impact toughness exhibited by PE16 on long-term ageing at 600 to 700° C [23] may well, therefore, be attributable to Laves phase formation.

Prior to the current work, M_6C has only been positively identified in PE16 following fast neutron irradiation at 535 and 630° C [3]. However, Mo–Si-rich particles, tentatively identified as M_6C, were detected by Bhanu Sankara Rao *et al.* [24] in 500 h/700° C aged PE16 using EDX/S (scanning) EM examinations of bulk samples. In fact it would be difficult to make a clear distinction between M_6C and Laves phase in the SEM because of matrix contributions to the EDX spectra. Positive identification of M_6C can be made by electron diffraction in the TEM but care is needed to differentiate it from $M_{23}C_6$. The lattice parameters of these two phases are very similar (Table II), but the diamond cubic structure of M_6C is distinguishable from the face-centred cubic (f c c) structure of $M_{23}C_6$ by the absence of {2 0 0} reflections in M_6C ⟨0 0 1⟩ zone axis diffraction patterns (Fig. 11).

Other phases which have been suggested to form on long-term ageing of PE16 are sigma phase [24] and M_7C_3 [25], but neither was found during this study. M_7C_3 was described as forming as needles or rosettes at sites within the grains on prolonged exposure at 500 to 750° C [25]. Its reported appearance is thus remarkably similar to that of intragranular Laves phase (Fig. 10), suggesting that it may perhaps have been mistakenly identified.

3.3. γ' Precipitation

The γ' phase, $Ni_3(Al, Ti)$, has an ordered f c c structure with a lattice parameter similar to that of the matrix

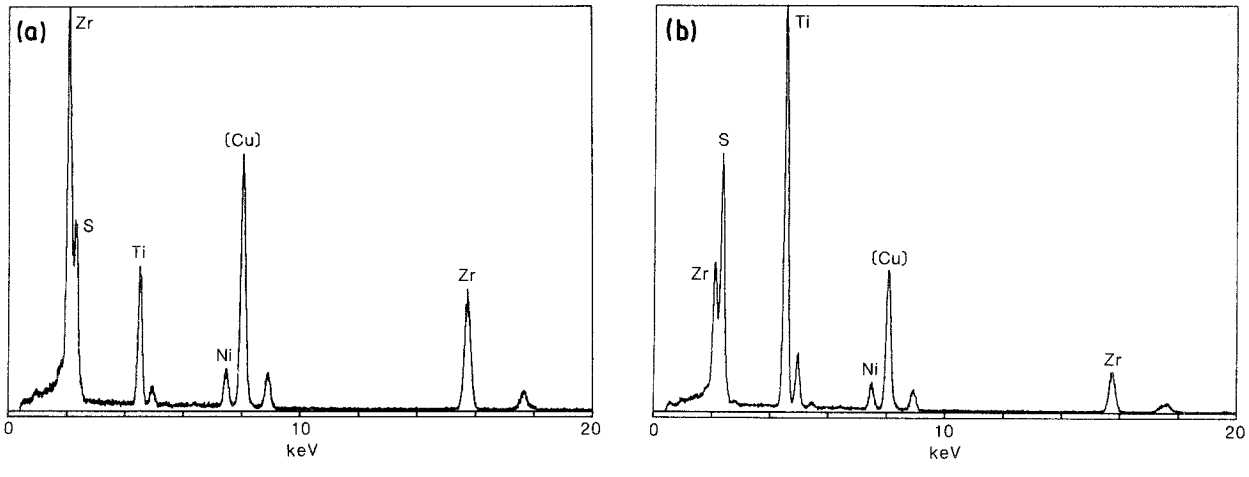

Figure 2 EDX spectra from (a) zirconium-rich and (b) titanium-rich $M_4C_2S_2$ particles.

TABLE III γ' precipitation data

T (°C)	t (h)	$\bar{d}$ (nm)	d_v (nm)	N_A (10^{13} m^{-2})	N_V (10^{20} m^{-3})	f (%)	d_b (nm)
850	240	134.2	140.6	0.233	0.173	2.52	–
800	1000	107.9	112.2	0.680	0.629	4.65	–
750	2	6.0	6.2	–	–	–	–
	4	8.9	9.3	54.9	615	2.57	–
	8	11.0	11.4	41.8	381	2.99	–
	16	11.6	12.2	44.3	383	3.61	–
	32	16.5	17.1	26.9	164	4.25	–
	64	19.3	20.3	17.9	97.3	4.07	35.3
	120	30.1	31.4	7.46	24.8	4.03	44.6
	240	35.6	37.7	6.52	18.3	5.14	51.3
	500	45.2	46.9	4.51	9.97	5.37	65.1
	1000	51.9	55.0	3.04	5.86	5.11	85.1
	2000	74.2	77.8	1.57	2.12	5.23	107.8
	4000	91.3	96.3	1.20	1.31	6.14	118.5
	6000	112.0	116.2	0.875	0.781	6.42	157.0
700	4000	31.6	33.2	10.2	32.3	6.21	–
650	4000	21.9	22.5	19.7	90.2	5.35	–

in PE16 and a solvus temperature of about 875° C. Precipitation of γ' was studied using replicas taken from ST specimens of PE16 aged isothermally at 650 to 850° C. A detailed assessment of the time dependence of precipitation was made at 750° C, together with measurements in the longest aged specimens at the other temperatures.

Evaluations of precipitate sizes and number densities were made from extraction and surface replicas, respectively. Examples of both type of γ' replica are shown in Fig. 12. In the preparation of both types of replica, the sample is first etched in oxalic acid. This results in matrix dissolution and the production of a new surface with unattacked γ' precipitates protruding from it. After carbon deposition the replica is stripped off by re-etching in either HCl/methanol or oxalic acid. In the former case, dissolution of both the matrix and γ' occurs so that only the precipitates which

TABLE IV Statistics* of γ' size distribution

T (°C)	t (h)	Standard deviation	Skew coefficient	Kurtosis
850	240	0.226	−0.315	2.941
800	1000	0.206	−0.320	2.788
750	2	0.196	0.418	3.015
	4	0.202	−0.018	2.880
	8	0.211	0.066	2.594
	16	0.236	−0.169	2.744
	32	0.196	−0.035	2.497
	64	0.234	0.034	2.672
	120	0.217	−0.232	2.521
	240	0.254	−0.356	2.529
	500	0.200	−0.582	3.265
	1000	0.258	−0.300	2.598
	2000	0.232	−0.489	3.221
	4000	0.235	−0.390	2.859
	6000	0.199	−0.352	3.237
700	4000	0.235	−0.574	2.957
650	6000	0.165	−0.181	2.844

*Standard deviation $= s = \left[\dfrac{\sum_{i=1}^{n}(x_i - 1)^2}{n}\right]^{1/2}$

where $x_i = (d_i/\bar{d})$;

skew coefficient $= \sum_{i=1}^{n}(x_i - 1)^3/ns^3$;

kurtosis (or peakedness) $= \sum_{i=1}^{n}(x_i - 1)^4/ns^4$

For a normal distribution the skew coefficient is zero and the kurtosis = 3. Positive and negative skewness indicate, respectively, that more than half of the data is less than and greater than the mean. For the LSW size distribution the standard deviation is 0.215, the skew coefficient −0.920 and the kurtosis 3.675.

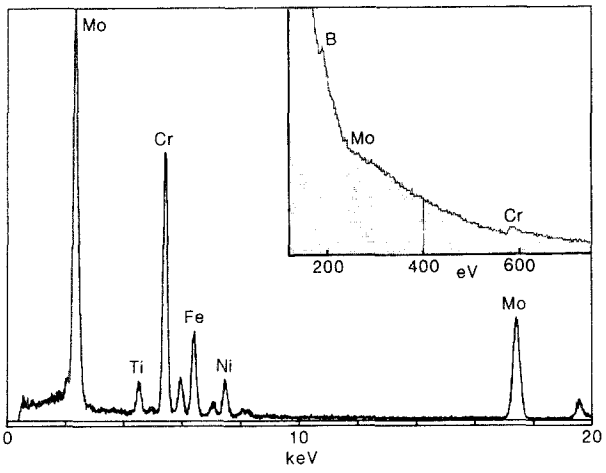

Figure 3 EDX and EEL spectra from M_3B_2.

intersected the first etched surface leave an impression in the carbon replica. In the latter case, only matrix dissolution occurs and γ' precipitates are extracted on to the replica. In practice the γ' is extracted not only from the first etched surface but also from some depth below it. This is shown by the fact that the number of extracted precipitates per unit area of replica is generally greater than the number per unit area in surface replicas. Also, the precipitates tend to agglomerate in extraction replicas, and electron diffraction reveals that the precipitates, which originally exhibit the same orientation as the matrix, become randomly oriented on extraction. Thus, the extraction process appears to be one of matrix dissolution freeing sub-surface γ' precipitates which then float off and become entrapped on the carbon film. It is therefore considered that the distribution of precipitate sizes measured on a γ' extraction replica is a reasonable approximation to the true volume distribution and that corrections for surface effects are unnecessary.

The results obtained for γ' size, number density and volume fraction are given in Table III. Statistical data for the size distributions are given in Table IV and compositional data (the Al/Ti atomic ratio in the precipitates) in Table V.

Precipitate coarsening can generally be represented by a relationship of the form $\bar{d} = kt^{\alpha}$, where t is time and k and α are constants. A plot of log ($\bar{d}$) against log (t) for the 750° C data yields a value for the time exponent α of 0.352 (with 95% confidence limits of ± 0.023). As in other nickel-base alloys [26], the growth rate of γ' in PE16 is consistent with the Lifshitz–Slyozov–Wagner (LSW) theory of diffusion-controlled coarsening which predicts $\alpha = 1/3$ [27, 28].

TABLE V Al/Ti atomic ratio in γ'

T (° C)	t (h)	Al/Ti ratio ($\pm$ standard deviation)	
		Intragranular γ'	Intergranular γ'
850	240	0.636 ± 0.025	0.563 ± 0.058
800	1000	0.715 ± 0.065	0.680 ± 0.064
750	240	0.903 ± 0.102	0.893 ± 0.068
	1000	0.822 ± 0.057	0.858 ± 0.077
	6000	0.837 ± 0.087	0.742 ± 0.101
700	4000	1.045 ± 0.068	1.176 ± 0.079
650	4000	1.120 ± 0.058	1.202 ± 0.042

The coarsening behaviour of grain boundary γ' was determined in specimens aged for 64 h or more at 750° C in which inter- and intra-granular precipitates could readily be distinguished. Extracted intergranular γ' precipitates are evident in Fig. 12a in which a grain boundary runs from the top right to bottom left corner. A log–log plot for coarsening of the grain boundary γ' gives a time exponent of 0.315 (95% confidence limits ± 0.031) again suggesting a $t^{1/3}$ dependence. This value may be compared with one of ~ 0.28 determined by Randle and Ralph in PE16 at 810° C [29]. Intuitively, a time exponent less than 1/3 for coarsening of intergranular γ' would not be expected because the sizes of precipitates in the matrix and at grain boundaries would then be converging.

Plots of γ' diameter ($\bar{d}$ and d_b) against $t^{1/3}$ are shown in Fig. 13, from which values of the rate constant k (in units of nm $h^{-1/3}$, with 95% confidence limits) are 6.07 ± 0.35 for intragranular precipitates and 8.05 + 1.11 for those at grain boundaries. For comparison with other published data a rate constant defined by $\bar{r}^3/t$, where $\bar{r}$ is the mean precipitate radius, is preferred. Values of this parameter (in units of $m^3 sec^{-1}$) are 7.76×10^{-30} for intragranular precipitates and 1.81×10^{-29} for grain-boundary precipitates. The rate constant for coarsening of intragranular γ' in

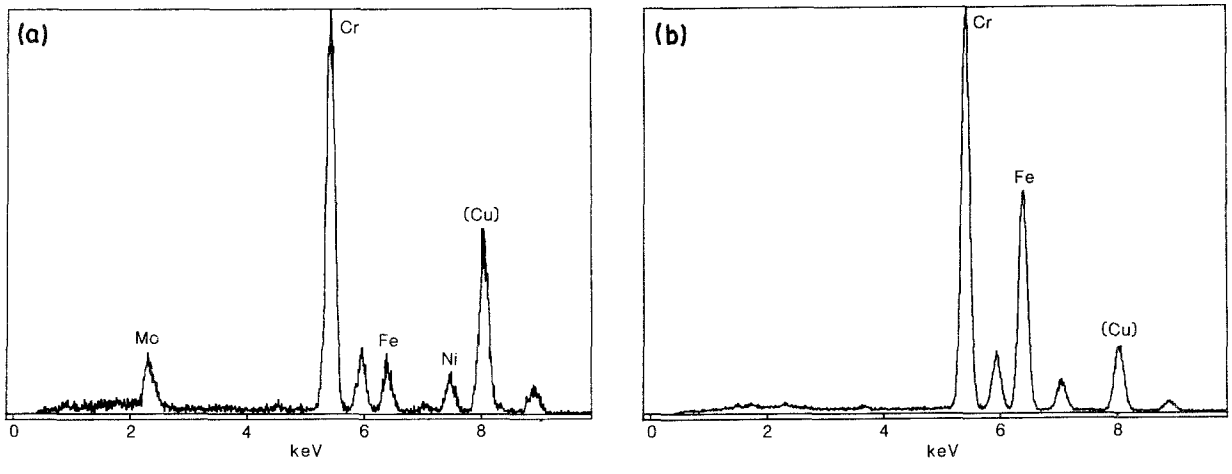

Figure 4 EDX spectra from $M_{23}C_6$ precipitates.

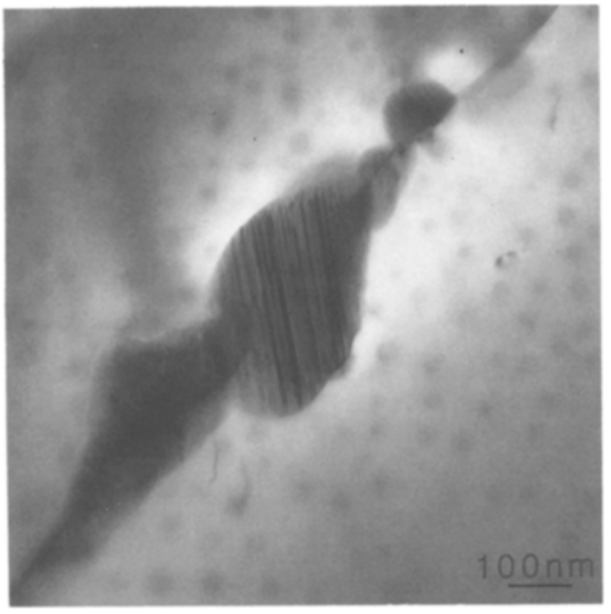

Figure 5 Grain-boundary Laves phase in PE16 aged 4000 h at 700° C.

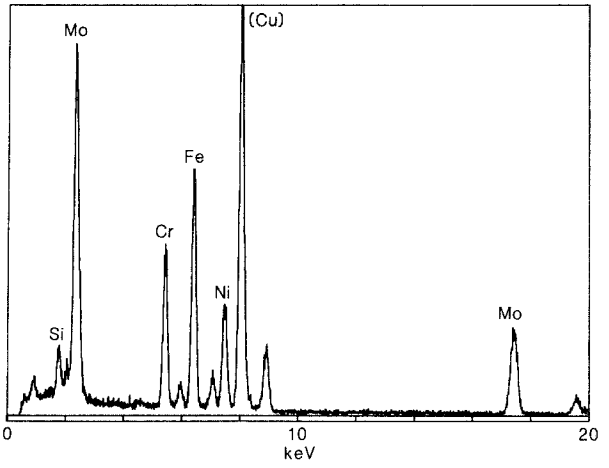

Figure 6 EDX spectrum from Laves phase.

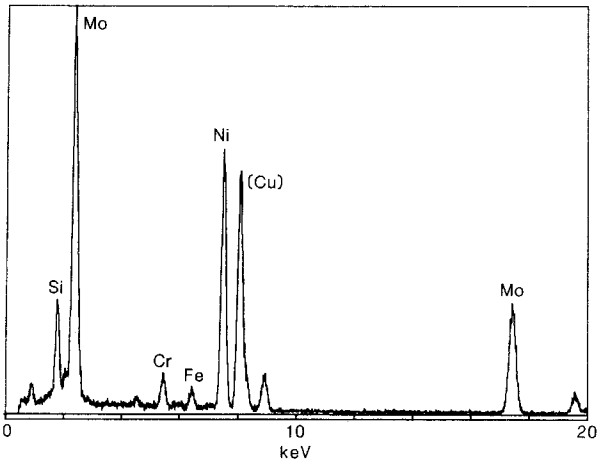

Figure 7 EDX spectrum from M_6C.

PE16 at 750° C is comparable to Gelles' result of 4.7×10^{-30} [2] but somewhat lower than the value of 2×10^{-29} found by Degischer *et al.* [9].

Regional variations in N_A amounted to standard deviations of typically 10%, giving rise to similar uncertainties in the derived values of N_V and f. The time exponent for the change in N_V during 750° C ageing is, from Fig. 14, -0.949 (95% confidence limits ± 0.079) which compares favourably with the value of -1 given by LSW. A straightforward plot of log (f) against log (t) shows that the γ' volume fraction increases during 750° C ageing with a time exponent of 0.109 (95% confidence limits ± 0.025). The time dependency of f is not given explicitly by LSW but the solute supersaturation is expected to decrease as $t^{-1/3}$ and this has been confirmed experimentally for binary Ni–Al alloys [30, 31]. A decreasing solute supersaturation implies an increasing volume fraction and Ardell [30] has shown that f approaches its equilibrium value f_e according to the relationship $(f_e - f) = \lambda t^{-1/3}$ where λ is a constant. Plotting f against $t^{-1/3}$, Fig. 15, gives a best estimate for the equilibrium volume fraction of γ' in PE16 at 750° C of 6.0%. This is similar to the values indicated by the work of Gelles [2] and Degischer *et al.* [9] at this temperature but significantly lower than the levels reported by Nembach and co-workers [1, 32, 33]. Only Gelles at 750° C [2] and Reppich *et al.* at higher temperatures [8] have previously observed the γ' volume fraction in PE16 to increase throughout the ageing period. Constant volume fractions at given ageing

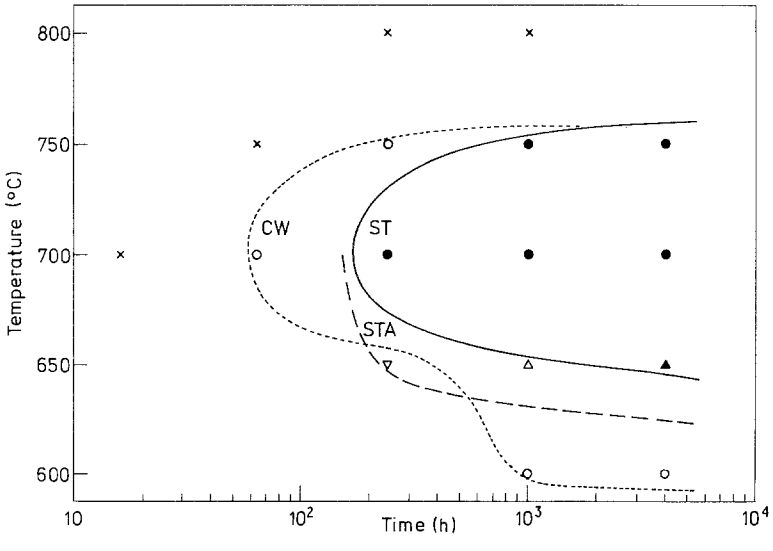

Figure 8 Time–temperature–precipitation diagram for Laves phase. (x) Laves not present. Laves present: (○) CW, (●) ST and CW, (▽) STA, (△) STA and CW, (▲) ST, STA and CW.

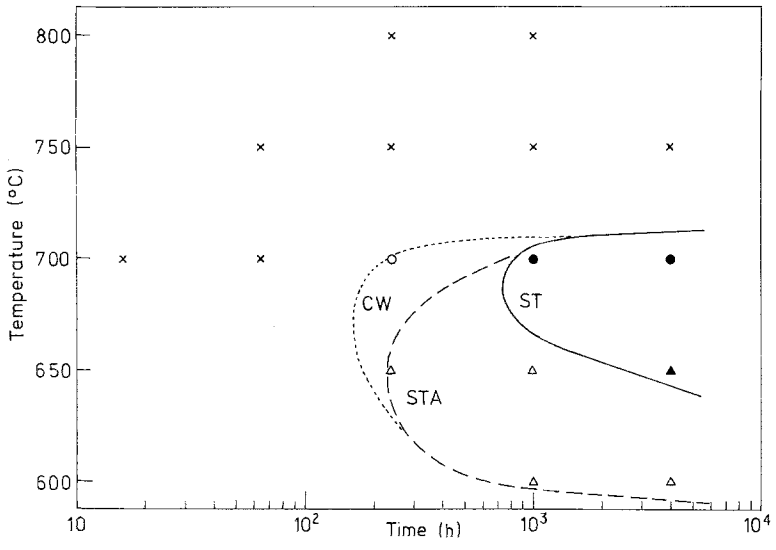

Figure 9 Time–temperature–precipitation diagram for M_6C. (x) M_6C not present. M_6C present: (○) CW, (●) ST and CW, (△) STA and CW, (▲) ST, STA and CW.

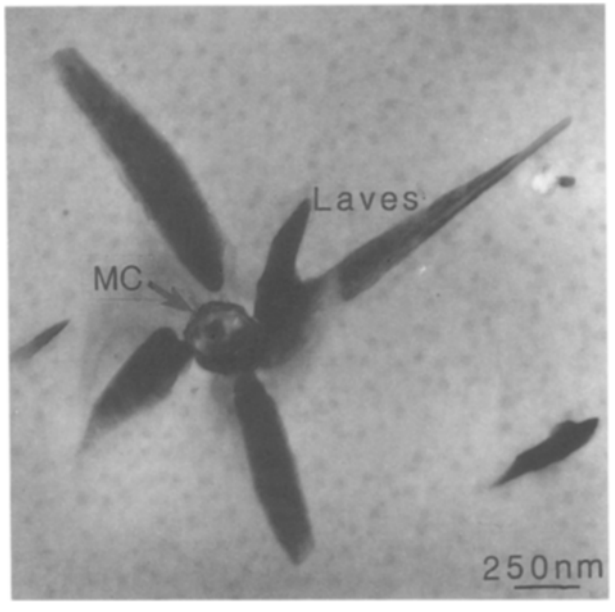

Figure 10 Intragranular precipitation of Laves phase in PE16 aged 4000 h at 700° C.

temperatures were reported by Degischer *et al.* and Nembach and co-workers, whereas Madden and Callen [7] found no further increase at times beyond 16 h at 700° C.

Although the time dependence of precipitate coarsening is predicted correctly by LSW theory, it is generally recognized that the precipitate size distribution is not. The reason for this is that LSW neglect precipitate interactions. Statistical analysis of the γ' size distributions in PE16 (Table IV) showed that the distributions were, in broad agreement with more recent models [34–38] and experimental data in other alloys, less skewed and less peaked than predicted by LSW. There is considerable scatter in the data but a change from a positive or near zero skew coefficient at ageing times up to 64 h at 750° C to negative skewness at longer times is evident. This change is attributable to the effect of coarsening on the initial size distribution produced by nucleation events. A typical example of the γ' size distribution in a long-term aged specimen of PE16, in which the distribution can be assumed to be

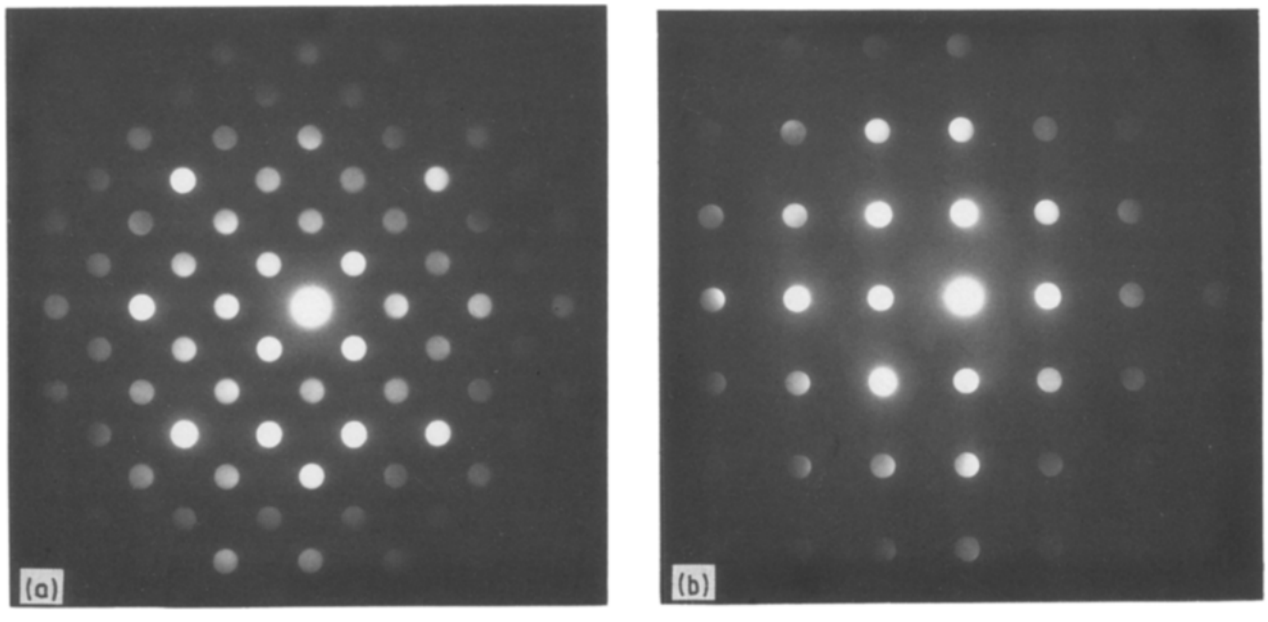

Figure 11 [0 0 1] zone axis convergent beam electron diffraction patterns from (a) $M_{23}C_6$ and (b) M_6C.

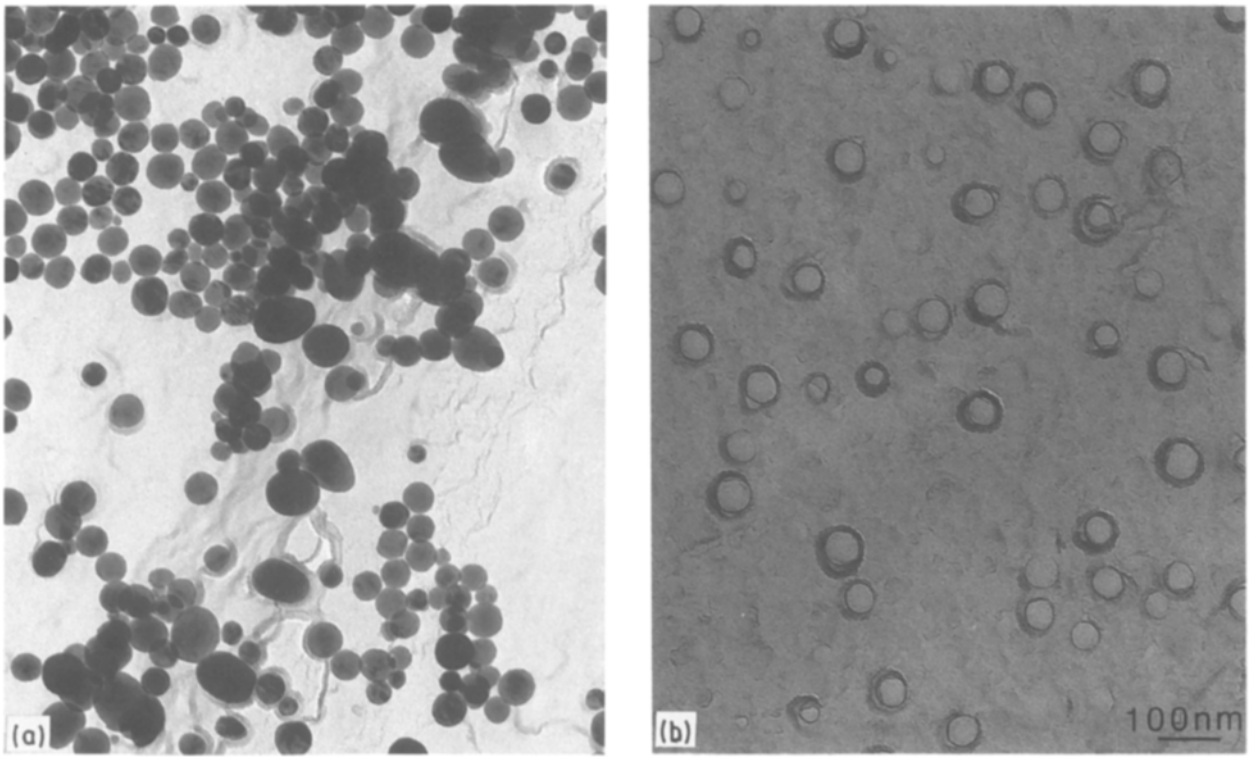

Figure 12 (a) γ' extraction replica and (b) γ' surface replica from PE16 aged 500 h at 750° C.

nearing steady-state, is shown in Fig. 16 with the LSW distribution for comparison.

There is some discrepancy in the literature over the composition of γ' in PE16, and it is unclear whether this reflects differences in analytical techniques, alloy composition and/or heat treatment. Mangen *et al.* [39] used EDX (Edax SW9100/60 system as in the present work) and EPMA and reported an average Al/Ti atomic ratio in γ' of 0.78. Degischer *et al.* [9] found a similar ratio using a field-ion atom probe. Other EDX data, however, indicate an Al/Ti atomic ratio of 1.4 to 1.7 [40, 41]. Moreover, Randle and Ralph [29, 42] have suggested, on the basis of lattice parameter measurements, that there may be a compositional difference between intragranular and grain boundary γ' in PE16. Although it is difficult to determine absolute compositions by EDX, particularly in the presence of light elements such as aluminium, careful application of the technique allows compositional changes to be followed. The data given in Table V reveal a clear trend of increasing Al/Ti ratio in γ' with decreasing ageing temperature but show much less significant variations between intragranular and grain-boundary precipitates. It is evident that the Al/Ti ratio in γ' only approaches the ratio of the atomic concentrations of these elements in PE16 as a

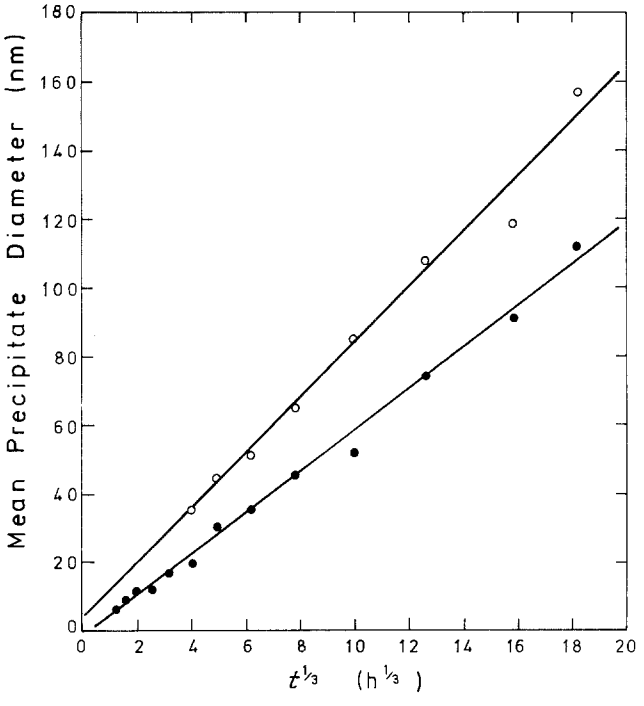

Figure 13 The variation in mean particle diameter with $t^{1/3}$, where t is time, for (●) intragranular and (○) grain boundary γ' in PE16 aged at 750° C.

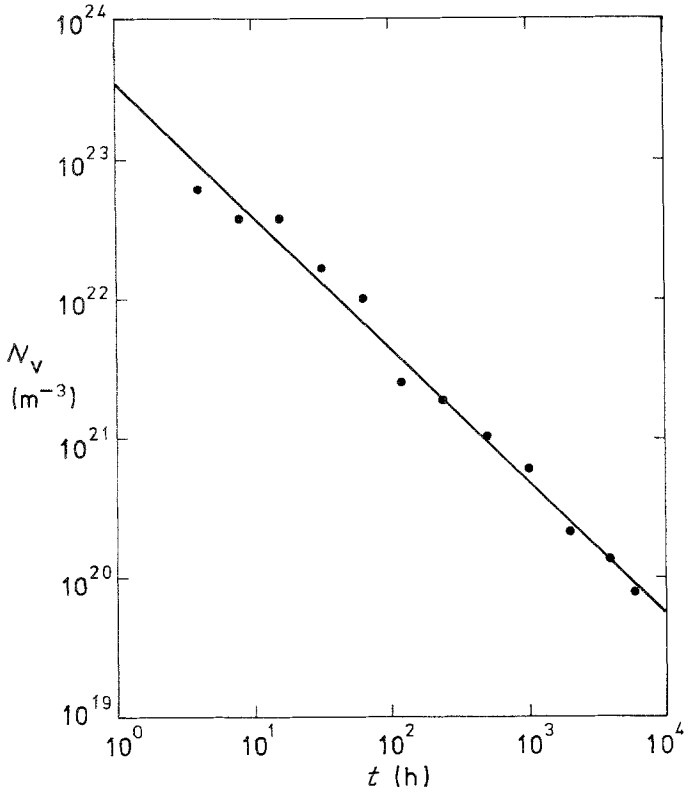

Figure 14 The variation in number of γ' precipitates per unit volume, N_V, with ageing time, t, for PE16 at 750° C.

whole (~2.4% Al, 1.4% Ti) at relatively low ageing temperatures.

4. Conclusions

1. The most abundant primary phases in Nimonic PE16 were found to be the (Ti, Mo)-rich carbide MC and the nitride TiN. Lesser amounts of $(Zr, Ti)_4C_2S_2$ and $(Mo, Cr)_3B_2$ were also present.

2. The chromium-rich carbide $M_{23}C_6$ precipitated at grain boundaries during isothermal ageing of PE16 at 850° C and below. $M_{23}C_6$ formed at 700° C was partially retained during subsequent annealing at 900° C but was fully dissolved at 950° C and above.

3. Precipitation of the (Mo, Fe, Si)-rich Laves phase occurred in PE16 during long-term exposure at 600 to 750° C. Precipitation occurred initially at grain boundaries and subsequently within the grains and was accelerated by cold working or pre-aging at 700° C prior to lower temperature exposure.

4. The (Mo, Ni, Si)-rich phase M_6C precipitated intergranularly in PE16 on long-term ageing at 600 to 700° C, and its formation was accelerated by cold working and pre-ageing at 700° C.

5. Quantitative assessments of γ' precipitation in PE16 have been made using extraction replicas to determine precipitate sizes and surface replicas for

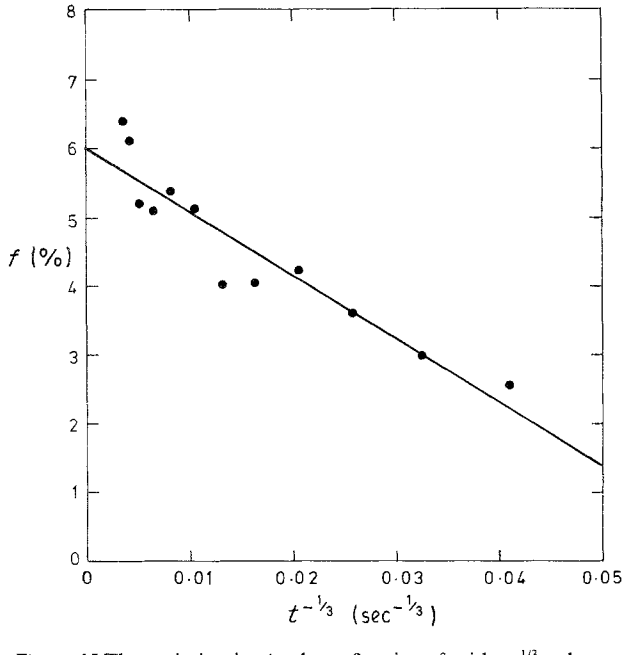

Figure 15 The variation in γ' volume fraction, f, with $t^{-1/3}$, where t is time, for PE16 aged at 750° C.

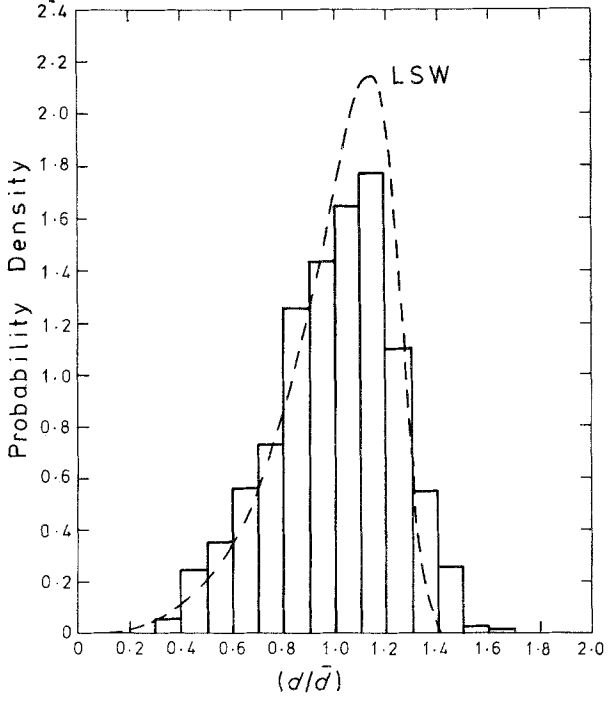

Figure 16 Comparison of measured γ' size distribution in PE16 aged 4000 h at 750° C with theoretical LSW distribution.

number densities. The variations in the mean diameter, $\bar{d}$, and the number of γ' precipitates per unit volume, N_V, with time, t, closely followed the $d \propto t^{1/3}$ and $N_V \propto t^{-1}$ relationships expected for diffusion-controlled coarsening. The volume fraction of γ' increased throughout the ageing period and approached an equilibrium value of about 6% at 750° C.

6. Coarsening of grain boundary γ' at 750° C also exhibited an approximate $t^{1/3}$ dependence.

7. The composition of γ' varied with ageing temperature, with the Al/Ti ratio increasing as the temperature decreased.

Acknowledgement

This work was undertaken as part of the Underlying Research Programme of the UKAEA. This paper is UKAEA copyright.

References

1. E. NEMBACH and G. NIETE, *Prog. Mater. Sci.* **29** (1985) 177.
2. D. S. GELLES, in Proceedings of the 10th International Conference on Effects of Radiation on Materials, ASTM STP 725, edited by D. Kramer, H. R. Brager and J. S. Perrin (ASTM, Philadelphia, Pennsylvania, 1981) p. 562.
3. R. M. BOOTHBY and D. R. HARRIES, in Proceedings of the International Conference on Mechanical Behaviour and Nuclear Applications of Stainless Steel at Elevated Temperatures, Varese, May 1981 (Metals Society, London, 1982) p. 157.
4. P. K. ROSE and V. M. CALLEN, in Proceedings of the BNES Conference on Nuclear Fuel Performance, Stratford-upon-Avon, March 1985 (British Nuclear Energy Society, London, 1985) p. 401.
5. R. M. BOOTHBY, *Met. Sci.* **13** (1979) 351.
6. V. RANDLE and B. RALPH, *Prak. Metallogr.* **22** (1985) 501.
7. P. K. MADDEN and V. M. CALLEN, *J. Mater. Sci.* **18** (1983) 3363.
8. B. REPPICH, W. KUHLEIN, G. MEYER, D. PUPPEL, M. SCHULZ and G. SCHUMANN, *Mater. Sci. Engng* **83** (1986) 45.
9. H. P. DEGISCHER, W. HEIN, H. STRECKER, W. WAGNER and R. P. WAHI, *Z. Metallkde* **78** (1987) 237.
10. E. E. UNDERWOOD, "Quantitative Stereology" (Addison-Wesley, Reading, Massachusetts, 1970) p. 96.
11. R. T. DeHOFF, in "Quantitative Microscopy', edited by R. T. DeHoff and F. N. Rhines (McGraw-Hill, New York, 1968) p. 128.
12. H. J. GOLDSCHMIDT, "Interstitial Alloys" (Butterworths, London, 1967) p. 536.
13. M. J. DONACHIE and O. H. KRIEGE, *J. Mater.* **7** (1972) 269.
14. J. MANSFIELD, "Convergent Beam Electron Diffraction of Alloy Phases" (Hilger, Bristol, 1984).
15. S. FLOREEN and J. M. DAVIDSON, *Metall. Trans. A* **14A** (1983) 895.
16. R. T. HOLT and W. WALLACE, *Int. Met. Rev.* **21** (1976) 1.
17. U. FRANZONI, F. MARCHETTI and S. STURLESE, *Scripta Metall.* **19** (1985) 511.
18. T. J. GAROSSHEN, T. D. TILLMAN and G. P. McCARTHY, *Metall. Trans. A* **18A** (1987) 69.
19. R. G. FAULKNER and J. CAISLEY, *Met. Sci.* **11** (1977) 200.
20. C. H. RICHARDSON, PhD thesis, University of Cambridge (1983).
21. R. M. BOOTHBY and G. B. MERRILL, in Proceedings 7th Risø International Symposium on Metallurgy and Materials Science, Annealing Processes – Recovery, Recrystallisation and Grain Growth, edited by N. Hansen, D. Juul Jensen, T. Leffers and B. Ralph (Risø National Laboratory, Roskilde, Denmark, 1986) p. 241.
22. C. T. SIMS, in "The Superalloys", edited by C. T. Sims and W. C. Hagel (Wiley, New York, 1972) p. 259.
23. G. B. STUBBS, in "The Nimonic Alloys", edited by W. Betteridge and J. Heslop (Arnold, London, 1974) p. 223.
24. K. BHANU SANKARA RAO, V. SEETHARAMAN, S. L. MANNAN and P. RODRIGUEZ, *Mater. Sci. Engng* **58** (1983) 93.
25. C. H. WHITE, in "The Nimonic Alloys", edited by W. Betteridge and J. Heslop (Arnold, London, 1974) p. 90.
26. D. McLEAN, *Met. Sci.* **18** (1984) 249.
27. I. M. LIFSHITZ and V. V. SLYOZOV, *J. Phys. Chem. Solids* **19** (1961) 35.
28. C. WAGNER, *Z. Elektrochem.* **65** (1961) 581.
29. V. RANDLE and B. RALPH, *Mater. Sci. Tech.* **3** (1987) 411.
30. A. J. ARDELL, in Proceedings of the Symposium on the Mechanisms of Phase Transformations in Crystalline Solids, Manchester, July 1968 (Institute of Metals, London, 1969) p. 111.
31. H. WENDT and P. HAASEN, *Acta Metall.* **31** (1983) 1649.
32. H. G. BRION and E. NEMBACH, *Phys. Status Solidi (a)* **26** (1974) 599.
33. V. MARTENS and E. NEMBACH, *Acta Metall.* **23** (1975) 149.
34. C. K. L. DAVIES, P. NASH and R. N. STEVENS, *ibid.* **28** (1980) 179.
35. K. TSUMURAYA and Y. MIYATA, *ibid.* **31** (1983) 437.
36. P. W. VOORHEES and M. E. GLICKSMAN, *ibid.* **32** (1984) 2013.
37. Y. ENOMOTO, K. KAWASAKI and M. TOKUYAMA, *ibid.* **35** (1987) 907.
38. *Idem, ibid.* **35** (1987) 915.
39. W. MANGEN, E. NEMBACH and H. SCHAFER, *Mater. Sci. Engng* **70** (1985) 205.
40. C. G. WINDSOR, V. S. RAINEY, P. K. ROSE and V. M. CALLEN, *J. Phys. F Met. Phys.* **14** (1984) 1771.
41. B. F. RILEY, E. G. WILSON and A. R. JONES, in Proceedings BNES Conference on Materials for Nuclear Reactor Core Applications, Bristol, October 1987, Vol. 2, (British Nuclear Energy Society, London, 1988) p. 17.
42. V. RANDLE and B. RALPH, *J. Microscopy* **147** (1987) 305.

Received 25 July
and accepted 22 November 1988